Engineering Notes

ENGINEERING NOTES are short manuscripts describing new developments or important results of a preliminary nature. These Notes cannot exceed 6 manuscript pages and 3 figures; a page of text may be substituted for a figure and vice versa. After informal review by the editors, they may be published within a few months of the date of receipt. Style requirements are the same as for regular contributions (see inside back cover).

AIAA 79-1879R

Spanwise Distribution of Control Points in the Method of Finite Elementary Solutions

Ji-Guang An*
Chinese Aerodynamic Research and Development Center, China

Nomenclature

C_L = lift coefficient
C_{Di} = induced drag coefficient
C_l = rolling moment coefficient
C.P. = control point
M = number of chordwise panels on half-wing
N = number of spanwise panels on half-wing
O = origin of coordinates
U = stream velocity, parallel to x axis
x,y = coordinate system, directions shown in Fig. 1
α = angle of attack
β = angle of yaw
δ = planform factor of induced drag
θ = angular coordinate
$\Delta\theta$ = angular interval
λ = aspect ratio

Introduction

IN the field of subsonic aerodynamics, the method of finite elementary solutions (vortex or doublet lattice method) has been one of the most broadly applied numerical methods. But in the computing of three-dimensional wing load distributions and aerodynamic characteristics, the results may vary as the number of spanwise lattices is changed. In the case of slender wings, the error of the lift-slope can be more than 2%, even with the number of spanwise lattices increased to 20.

The computation of induced drag is probably the most troublesome problem in potential flow solutions because it requires a very accurate calculation of the lift distribution.

In former method of finite elementary solutions (MFES) programs, this problem remains unsolved. In Ref. 1, Shiang had reviewed the various methods published for induced drag calculation. For planar lifting surfaces with simple planforms, the classic methods, such as lifting line and lifting surface theory, are sufficient to obtain good results. As the wing geometry becomes more complex, e.g., with arbitrary planform and camber, one must rely on numerical methods such as the MFES.

In Chap. 10 of Ref. 2, three possible ways to calculate the induced drag using the MFES were investigated, namely: 1) through the calculation of wing leading edge suction; 2) through the calculation of ideal angle of attack (design angle of attack) of each chordwise strip; and 3) by means of combined flow theory. The last is probably the most efficient way, but demands a very accurate computation of spanwise load distribution.

Presented as Paper 79-1879 at the AIAA Aircraft Systems and Technology Meeting, New York, N.Y., Aug. 20-22, 1979; submitted Sept. 17, 1979; revision received June 25, 1980.

*Senior engineer.

Midpanel Locations of Control Points

The chordwise locations of control points, were studied before 1972,[3,4] and the effects of spanwise deviations of control points from midpanel points were investigated later.[5] In general applications, the choice of spanwise locations was rather intuitive, the midpanel point (both chordwise and spanwise) or the geometric centroid of lattice panel[5] was designated as the proper location of control point, and the results of lift and pitching moment characteristics were considered good.

As the calculation of induced drag is performed, however, the midpanel control point arrangement is rather inadequate. The calculated planform factor

$$\delta = C_{Di}(\pi\lambda/C_L^2) - 1 \tag{1}$$

is always negative, which means the calculated induced drags are smaller than the theoretical minimum. For most wing planforms, the inaccurate results still persist even with a large increase in the number of spanwise panels.

For slender wings with small aspect ratio, the lift errors arising from midpanel control points are more pronounced along with the induced drag errors. From slender wing theory, one obtains

$$\frac{2C_L}{\pi\lambda\alpha} = 1$$
$$\delta = 0 \tag{2}$$

In the case of the number of chordwise panels $M=1$, for various numbers of spanwise panels N (on half of a span), calculations by means of the MFES using midpanel C.P. can be summarized in the following formulas:

$$\frac{2C_L}{\pi\lambda\alpha} = 1 + \frac{1}{2N}$$
$$\delta = \frac{2N}{2N+1} - 1 \tag{3}$$

The lift-slope increases with spanwise panel number N, and monotonically approaches its exact value. In the worst condition of $N=0.5$, the error reaches 100%.

Table 1 shows the calculated results of a rectangular wing of aspect ratio 2 using the MFES with midpanel C.P.; all the planform factors δ are negative even with the spanwise panel number increased to 60. The chordwise panel number M may differ from 1, but has only a minor effect on calculated results.

Table 1 Comparison between $M=1$ and $M>1$, MFES results using midpanel C.P. for a $\lambda=2$ rectangular wing

	Planform factor of induced drag δ	
No. of semi-span panels N	Chordwise panels No. $M=1$	Chordwise panels No. $M>1$[a]
5	−0.0909	−0.0902 (24)
6	−0.0770	−0.0763 (20)
8	−0.0588	−0.0581 (10)
15	−0.0323	−0.0316 (10)
24	−0.0204	−0.0198 (5)
30	−0.0164	−0.0158 (4)
60	−0.0082	−0.0077 (2)

[a] Numbers in parentheses are M values.

Table 2 Planform factors calculated by MFES with midpanel C.P. for various planform wings, panel division $MxN=10\times15$

Wing planform	Aspect ratio λ	Planform factor of induced drag δ
Rectangular	1	−0.0323
	3	−0.0296
	6	−0.0162
28.5 deg swept (no taper)	1	−0.0515
	2	−0.0438
	3	−0.0339
	4	−0.0215
45- deg swept (no taper)	1	−0.0567
	3	−0.0125
	5	−0.0383
60- deg triangular	2.31	−0.0660
Elliptic (unswept)	5.34	−0.0864

Table 3 Calculated results of MFES using projected C.P. for rectangular wings of aspect ratio 2 and 6

Aspect ratio λ	Chordwise panels × spanwise panels $M\times N$	Lifting curve slope C_L^α	Induced drag factor δ
2	10 × 15	2.4738	0.00065
	10 × 12	2.4738	0.00065
	10 × 5	2.4735	0.00067
	10 × 15	2.4738	0.00065
	6 × 15	2.4729	0.00064
	4 × 15	2.4711	0.00063
	8 × 8	2.4735	0.00065
6	10 × 15	4.2141	0.01642
	10 × 5	4.2115	0.01697

Table 4 Planform factors calculated by MFES with projected C.P. for various planform wings, panel division $M\times N=10\times15$

Wing planform	Aspect ratio λ	Planform factor of induced drag δ
Rectangular	1	0.00002
	3	0.00271
	10	0.04218
28.5- deg swept (no taper)	1	0.00019
	3	0.01392
	6	0.05689
45- deg swept (no taper)	1	0.00070
	3	0.04062
	6	0.12185
Triangular[a]	2.31	0.01578
	4	0.03856
	6.93	0.08120

[a] The leading edge swept angle of these three triangular wings are 60, 45, and 30 deg, respectively.

In addition to these results, we had calculated some planar wings with different planforms to illustrate the inadequacy of the MFES while using midpanel C.P. The total number of panels was $M\times N=10\times15=150$. The calculated planform factors are tabulated in Table 2. It may be concluded that the correct induced drag can not be obtained with the traditional midpanel control point locations.

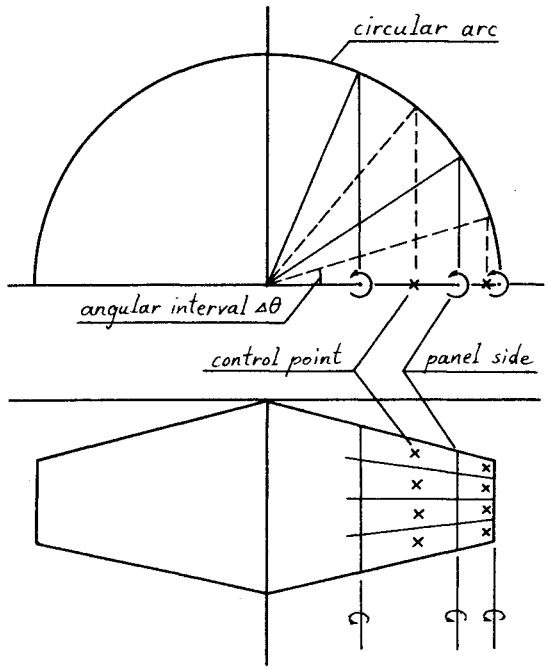

Fig. 1 Projected arrangement of panel sides (mesh lines) and control points.

Projected Spanwise Location of Control Points

In 1976, An[6] suggested the so-called projected spanwise locations of control points. With this projected C.P. and correlated panel divisions, the MFES becomes an accurate tool for induced drag calculations. The calculated lift coefficient C_L and planform factor δ are very accurate even with a small number of spanwise panels. Furthermore, the overload phenomena at wing tip regions which are the inherent errors of midpanel C.P. are eliminated also.

Figure 1 shows the general arrangement. Angular interval $\Delta\theta$ is a constant determined by

$$\Delta\theta=\pi/4N \tag{4}$$

The rays with angular intervals $\Delta\theta$ intersect the semicircle which has a radius of semispan, then the projections of these intersections on the y axis are the panel sides (mesh lines) and control points alternately.

A slender wing was calculated by means of the optimum C.P., chordwise panel number $M=1$, and spanwise panel number varied from 1 to 30. All these calculations gave the exact results of C_L and δ, as shown by Eq. (2).

In order to examine the sensitivity of calculated results with projected C.P. locations to the number of panels $M\times N$, two rectangular wings of aspect ratio 2 and 6 were computed. The results are tabulated in Table 3. Whatever the panel number or panel scale $M\times N$ are, lift curve slope C_L^α and planform factor of induced drag δ remain nearly unchanged as anticipated.

Table 4 presents the calculated results by means of projected C.P. for wings of various planforms. When Shiang had computed the induced drags of wings with cranked leading edge,[1] the results were very good too.

Huang[7] investigated the application of MFES to the calculation of yawed wings. He found that the projected C.P. was superior to midpanel C.P. in both accuracy and convergence. Table 5 shows the rolling moment derivative C_l^β of an untapered 45-deg swept planar wing ($\lambda=2.61$) computed by the MFES with both projected and midpanel C.P. For various panel divisions calculated, the maximum error of projected C.P. was less than 1%, but that of midpanel C.P. exceeded 4%.

Table 5 Rolling moment derivatives C_l^β/C_L of an untapered 45-deg swept plane wing (aspect ratio $\lambda = 2.61$) as computed by MFES

Chordwise panels × spanwise panels $M \times N$	C_l^β/C_L	
	Projected C.P.	Midpanel C.P.
2 × 2	−0.4941	−0.5236
2 × 8	−0.4971	−0.5045
2 × 16	−0.4981	−0.5012
4 × 4	−0.4932	−0.5095
4 × 8	−0.4928	−0.5002
6 × 6	−0.4910	−0.5025

In Chiao's computation[8] of nonlinear vortex lift based on Polhamus' suction analogy, he recommended that the projected C.P. was the best arrangement of MFES to calculate suction forces acting on wing side edges.

DeJarnette[9] had treated the problem of spanwise distribution of control points in 1976. In his paper, the present projected C.P. distribution was called "conventional" and was quoted to have the same unsatisfied results as the midpanel C.P. arrangement. He had proposed another C.P. arrangement which was almost identical with ours except the positions of panel side and control point were interchanged. But, our work on this subject has already shown that the projected C.P. arrangement is far from "conventional," it behaves more superior to the midpanel C.P. When compared with DeJarnette's, the projected C.P. provides the same accuracy and rate of convergence.

References

[1] Shiang, Y.S., "The Calculation of Wing Induced Drag in Subsonic Flow," CARDC unpublished paper, June 1977.

[2] An, J.G., "The Method of Finite Elementary Solutions in Subsonic Aerodynamics," *CARDC Aerodynamic Research and Development,* No. 7, May 1977, p. 52.

[3] An, J.G., "The Control Point Locations of MFES in the Calculation of Two-Dimensional Thin Wings," CARDC unpublished paper, Nov. 1970.

[4] An, J.G., "The Problem of Lattice Division for the Numerical Solution of Two-Dimensional Plane Wing," CARDC unpublished paper, Nov. 1971.

[5] An, J.G., "The Problem of Control Point Distribution in Three-Dimensional Wing Calculations," CARDC unpublished paper, Oct. 1971.

[6] An, J.G., "The Spanwise Locations of Control Points in MFES for Subsonic Wings and the Problem of Induced Drag," *Journal of CARDC,* No. 1, 1977, p. 1.

[7] Huang, G.C., "The Calculation of Lateral Aerodynamic Characteristics of Subsonic Thin Wings," *Journal of CARDC,* No. 1, 1979, p. 21.

[8] Chiao, S.H., "Nonlinear Subsonic Aerodynamic Calculation of Aircraft with Small Aspect Ratio Wings," to be published in *Journal of CARDC,* p. 21.

[9] DeJarnette, F.R., "Arrangement of Vortex Lattices," presented at "Vortex-Lattice Utilization," NASA SP-405, N76-28180, May 1976.

AIAA 81-4026

Aerodynamics of a Round Jet in a Counterflowing Wind

Robert E. Peck*

University of Kentucky, Lexington, Ky.

Introduction

FLOWS involving the interaction of a circular jet and an unconfined, opposing stream may be encountered during V/STOL, thrust reversal, or dispersive operations. Limited information about these complex flows has thus far been obtained from a few experimental[1-4] and analytical[5-7] studies. This Note presents and appraises a numerical model of the flowfield.

The flow configuration and pertinent physical quantities are shown in Fig. 1. An incompressible, turbulent jet of diameter d_j and velocity U_j discharges into an expansive, uniform velocity (U_∞) counterflow of the same fluid. The backward deflection of the jet by the opposing stream generates a highly turbulent flowfield characterized by a large stationary recirculation zone along the periphery of the jet.

Mathematical Model

The numerical analysis of the flowfield is accomplished by simultaneously solving the governing time-averaged differential equations for mass, momentum, and turbulence properties listed in the following equations.

$$\frac{\partial}{\partial x_i}(\rho U_i) = 0 \tag{1}$$

$$\frac{\partial}{\partial x_i}(\rho U_i U_j) = -\frac{\partial p}{\partial x_i} + \frac{\partial \tau_{ij}}{\partial x_i} \tag{2}$$

$$\frac{\partial}{\partial x_i}(\rho U_i k) = \frac{\partial}{\partial x_i}\left(\frac{\mu_{\text{eff}}}{\sigma_k}\frac{\partial k}{\partial x_i}\right) + G - \rho\epsilon \tag{3}$$

$$\frac{\partial}{\partial x_i}(\rho U_i \epsilon) = \frac{\partial}{\partial x_i}\left(\frac{\mu_{\text{eff}}}{\sigma_\epsilon}\frac{\partial \epsilon}{\partial x_i}\right) + \frac{\epsilon}{k}\left(c_1 G - c_2 \rho\epsilon\right) \tag{4}$$

where

$$\tau_{ij} = -\rho\overline{u_i u_j} = \mu_{\text{eff}}\left(\frac{\partial U_i}{\partial x_j} + \frac{\partial U_j}{\partial x_i}\right) - \frac{2}{3}\rho k \delta_{ij}$$

$$\mu_{\text{eff}} = c_\mu \rho k^2/\epsilon, \qquad k = \tfrac{1}{2}\overline{u_i u_i}$$

$$\epsilon = \nu(\partial \bar{u}_i/\partial x_j)^2, \qquad G = -\rho\overline{u_i u_j}\,\partial U_i/\partial x_j$$

The constants appearing in the preceding equations are $\sigma_k = 1.0$, $\sigma_\epsilon = 1.22$, $c_\mu = 0.09$, $c_1 = 1.44$, and $c_2 = 1.92$. A detailed description of the two-equation k-ϵ (kinetic energy-dissipation rate) turbulence model adopted for this work may be found in Ref. 8.

The model also prescribes conditions at the periphery of the open, axisymmetric flowfield. Along the symmetry axis ($r = 0$), $V = 0$, and $\partial/\partial r$ of all other variables $= 0$. $\partial/\partial x$ of all variables $= 0$ at the exit plane and as $r \to \infty$, all properties conform to freestream conditions. The values of $U, V, p, k,$ and ϵ are assigned at the jet and freestream inlet planes.

The computational procedure used to solve the above set of equations in conjunction with specified boundary conditions

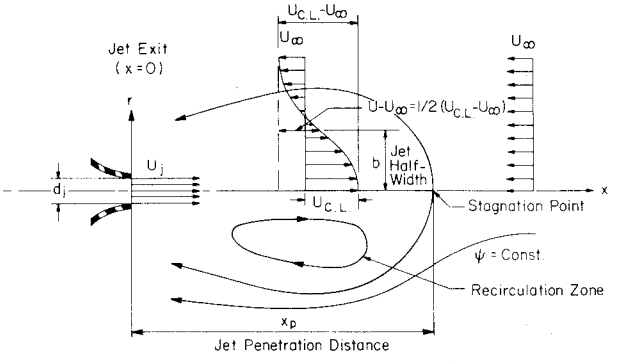

Fig. 1 Flowfield schematic.

Received June 10, 1980.

*Assistant Professor, Dept. of Mechanical Engineering.